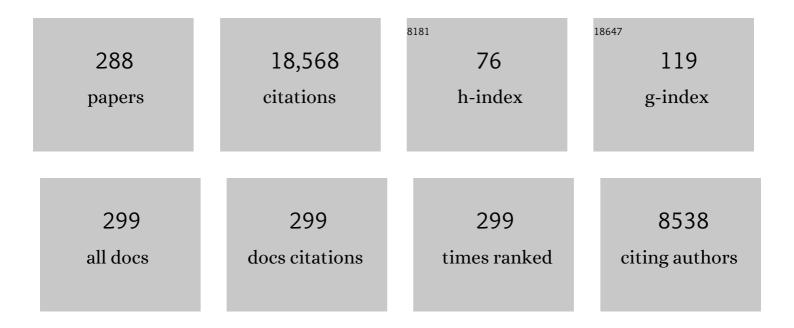
## Chun-Zhu Li

List of Publications by Year in descending order

Source: https://exaly.com/author-pdf/7042883/publications.pdf Version: 2024-02-01



Сним-7ни Ц

#	Article	IF	CITATIONS
1	An integrated two-step process of reforming and adsorption using biochar for enhanced tar removal in syngas cleaning. Fuel, 2022, 307, 121935.	6.4	18
2	Cross-polymerization between the model furans and phenolics in bio-oil with acid or alkaline catalysts. Green Energy and Environment, 2021, 6, 138-149.	8.7	13
3	Kinetic features of ethanol steam reforming and decomposition using a biochar-supported Ni catalyst. Fuel Processing Technology, 2021, 212, 106622.	7.2	27
4	High-pressure reactive distillation of bio-oil for reduced polymerisation. Fuel Processing Technology, 2021, 211, 106590.	7.2	20
5	In situ SAXS studies of the pore development in biochar during gasification. Carbon, 2021, 172, 454-462.	10.3	24
6	Reactions and Distribution of Levoglucosan during the High-Pressure Reactive Distillation of Bio-Oil. Industrial & Engineering Chemistry Research, 2021, 60, 6298-6305.	3.7	5
7	A SAXS study of the pore structure evolution in biochar during gasification in H2O, CO2 and H2O/CO2. Fuel, 2021, 292, 120384.	6.4	25
8	Insights into the mechanism of tar reforming using biochar as a catalyst. Fuel, 2021, 296, 120672.	6.4	24
9	Enrichment of aromatic compounds during the high-pressure reactive distillation of bio-oil. Fuel Processing Technology, 2021, 220, 106897.	7.2	7
10	Conversion of carbonyl compounds in bio-oil during the acid/base-catalysed reactive distillation at high pressure. Fuel, 2021, 304, 121492.	6.4	4
11	Studies into the kinetic compensation effects of Loy Yang Brown coal during gasification in a steam environment – A mechanistic view. Chemical Engineering Journal Advances, 2021, 8, 100159.	5.2	11
12	Polymerization of sugars/furan model compounds and bio-oil during the acid-catalyzed conversion – A review. Fuel Processing Technology, 2021, 222, 106958.	7.2	12
13	Mechanistic Insights into the Kinetic Compensation Effects during the Gasification of Loy Yang Brown Coal Char in O <sub>2</sub> . Industrial & Engineering Chemistry Research, 2021, 60, 17881-17896.	3.7	6
14	Mechanistic insights into the kinetic compensation effects during the gasification of biochar: Effects of the partial pressure of H2O. Fuel, 2020, 263, 116632.	6.4	10
15	Difference in tar reforming activities between biochar catalysts activated in H2O and CO2. Fuel, 2020, 271, 117636.	6.4	26
16	Microkinetic modelling and reaction pathway analysis of the steam reforming of ethanol over Ni/SiO2. International Journal of Hydrogen Energy, 2019, 44, 22816-22830.	7.1	17
17	Hydrotreatment of pyrolysis bio-oil: A review. Fuel Processing Technology, 2019, 195, 106140.	7.2	146
18	Mechanistic insights into the kinetic compensation effects during the gasification of biochar in H2O. Fuel, 2019, 255, 115839.	6.4	14

Chun-Zhu Li

#	Article	IF	CITATIONS
19	High yields of solid carbonaceous materials from biomass. Green Chemistry, 2019, 21, 1128-1140.	9.0	103
20	Role of O-containing functional groups in biochar during the catalytic steam reforming of tar using the biochar as a catalyst. Fuel, 2019, 253, 441-448.	6.4	104
21	Steam reforming of guaiacol over Ni/Al2O3 and Ni/SBA-15: Impacts of support on catalytic behaviors of nickel and properties of coke. Fuel Processing Technology, 2019, 191, 138-151.	7.2	78
22	Investigation into the Flow Assurance of Waxy Crude Oil by Application of Graphene-Based Novel Nanocomposite Pour Point Depressants. Energy & Fuels, 2019, 33, 12330-12345.	5.1	30
23	A case study: what is leached from mallee biochars as a function of pH?. Environmental Monitoring and Assessment, 2018, 190, 294.	2.7	9
24	An X-ray photoelectron spectroscopic perspective for the evolution of O-containing structures in char during gasification. Fuel Processing Technology, 2018, 172, 209-215.	7.2	16
25	Oxidative pyrolysis of mallee wood biomass, cellulose and lignin. Fuel, 2018, 217, 382-388.	6.4	44
26	Destruction of tar during volatile-char interactions at low temperature. Fuel Processing Technology, 2018, 171, 215-222.	7.2	68
27	Acid-treatment of bio-oil in methanol: The distinct catalytic behaviours of a mineral acid catalyst and a solid acid catalyst. Fuel, 2018, 212, 412-421.	6.4	26
28	Changes in char structure during the low-temperature pyrolysis in N2 and subsequent gasification in air of Loy Yang brown coal char. Fuel, 2018, 212, 187-192.	6.4	41
29	Changes in the Biochar Chemical Structure during the Low-Temperature Gasification of Mallee Biochar in Air as Revealed with Fourier Transform Infrared/Raman and X-ray Photoelectron Spectroscopies. Energy & Fuels, 2018, 32, 12545-12553.	5.1	7
30	Kinetic compensation effects in the chemical reaction-controlled regime and mass transfer-controlled regime during the gasification of biochar in O2. Fuel Processing Technology, 2018, 181, 25-32.	7.2	23
31	Reaction behaviour of light and heavy components of bio-oil in methanol and in water. Fuel, 2018, 232, 645-652.	6.4	6
32	Effects of the Particle Size and Gasification Atmosphere on the Changes in the Char Structure during the Gasification of Mallee Biomass. Energy & Fuels, 2018, 32, 7678-7684.	5.1	14
33	A self-heating oxygen pump using microchanneled ceramic membranes for portable oxygen supply. Chemical Engineering Science, 2018, 192, 541-550.	3.8	4
34	High performance anode with dendritic porous structure for low temperature solid oxide fuel cells. International Journal of Hydrogen Energy, 2018, 43, 17849-17856.	7.1	18
35	Nanocatalysts anchored on nanofiber support for high syngas production via methane partial oxidation. Applied Catalysis A: General, 2018, 565, 119-126.	4.3	16
36	Evolution of structure and activity of char-supported iron catalysts prepared for steam reforming of bio-oil. Fuel Processing Technology, 2017, 158, 180-190.	7.2	41

#	Article	IF	CITATIONS
37	Pyrolysis of large mallee wood particles: Temperature gradients within a pyrolysing particle and effects of moisture content. Fuel Processing Technology, 2017, 158, 163-171.	7.2	33
38	Effects of char chemical structure and AAEM retention in char during the gasification at 900 °C on the changes in low-temperature char-O 2 reactivity for Collie sub-bituminous coal. Fuel, 2017, 195, 253-259.	6.4	23
39	Effects of gasification temperature and atmosphere on char structural evolution and AAEM retention during the gasification of Loy Yang brown coal. Fuel Processing Technology, 2017, 159, 48-54.	7.2	40
40	One-pot conversion of biomass-derived xylose and furfural into levulinate esters via acid catalysis. Chemical Communications, 2017, 53, 2938-2941.	4.1	82
41	Effects of thermal pretreatment and ex-situ grinding on the pyrolysis of mallee wood cylinders. Fuel Processing Technology, 2017, 159, 211-221.	7.2	10
42	Changes in char structure during the thermal treatment of nascent chars in N 2 and subsequent gasification in O 2. Fuel, 2017, 199, 264-271.	6.4	21
43	Grinding pyrolysis of Mallee wood: Effects of pyrolysis conditions on the yields of bio-oil and biochar. Fuel Processing Technology, 2017, 167, 215-220.	7.2	32
44	Hierarchically ordered porous Ni-based cathode-supported solid oxide electrolysis cells for stable CO <sub>2</sub> electrolysis without safe gas. Journal of Materials Chemistry A, 2017, 5, 24098-24102.	10.3	35
45	Effects of calcination temperature of electrospun fibrous Ni/Al 2 O 3 catalysts on the dry reforming of methane. Fuel Processing Technology, 2017, 155, 246-251.	7.2	52
46	Upgrading of bio-oil via acid-catalyzed reactions in alcohols — A mini review. Fuel Processing Technology, 2017, 155, 2-19.	7.2	95
47	Biofuel and Methyl Levulinate from Biomassâ€Derived Fractional Condensed Pyrolysis Oil and Alcohol. Energy Technology, 2017, 5, 205-215.	3.8	5
48	Coke formation during the hydrotreatment of bio-oil using NiMo and CoMo catalysts. Fuel Processing Technology, 2017, 155, 261-268.	7.2	53
49	Effects of Alkali and Alkaline Earth Metallic Species and Chemical Structure on Nascent Char–O <sub>2</sub> Reactivity. Energy & Fuels, 2017, 31, 13578-13584.	5.1	11
50	Thin ceramic membrane with dendritic microchanneled sub structure and high oxygen permeation rate. Journal of Membrane Science, 2017, 541, 653-660.	8.2	17
51	Effects of water and alcohols on the polymerization of furan during its acid-catalyzed conversion into benzofuran. RSC Advances, 2016, 6, 40489-40501.	3.6	34
52	Feasibility of tubular solid oxide fuel cells directly running on liquid biofuels. Chemical Engineering Science, 2016, 154, 108-118.	3.8	27
53	Microchannel structure of ceramic membranes for oxygen separation. Journal of the European Ceramic Society, 2016, 36, 3193-3199.	5.7	16
54	Effects of temperature on the hydrotreatment behaviour of pyrolysis bio-oil and coke formation in a continuous hydrotreatment reactor. Fuel Processing Technology, 2016, 148, 175-183.	7.2	77

#	Article	IF	CITATIONS
55	Improved gas diffusion within microchanneled cathode supports of SOECs for steam electrolysis. International Journal of Hydrogen Energy, 2016, 41, 19829-19835.	7.1	34
56	Formation of aromatic ring structures during the thermal treatment of mallee wood cylinders at low temperature. Applied Energy, 2016, 183, 542-551.	10.1	16
57	Formation of coke during the esterification of pyrolysis bio-oil. RSC Advances, 2016, 6, 86485-86493.	3.6	20
58	Importance of hydrogen and bio-oil inlet temperature during the hydrotreatment of bio-oil. Fuel Processing Technology, 2016, 150, 132-140.	7.2	36
59	An advanced biomass gasification technology with integrated catalytic hot gas cleaning. Part III: Effects of inorganic species in char on the reforming of tars from wood and agricultural wastes. Fuel, 2016, 183, 177-184.	6.4	64
60	Different reaction behaviours of the light and heavy components of bio-oil during the hydrotreatment in a continuous pack-bed reactor. Fuel Processing Technology, 2016, 146, 76-84.	7.2	34
61	Simultaneous hydrogenation and acid-catalyzed conversion of the biomass-derived furans in solvents with distinct polarities. RSC Advances, 2016, 6, 4647-4656.	3.6	26
62	Feasibility of Direct Utilization of Biomass Gasification Product Gas Fuels in Tubular Solid Oxide Fuel Cells for On-Site Electricity Generation. Energy & Fuels, 2016, 30, 1849-1857.	5.1	29
63	Polymerization and cracking during the hydrotreatment of bio-oil and heavy fractions obtained by fractional condensation using Ru/C and NiMo/Al2O3 catalyst. Journal of Analytical and Applied Pyrolysis, 2016, 118, 136-143.	5.5	43
64	Structural transformation of nascent char during the fast pyrolysis of mallee wood and low-rank coals. Fuel Processing Technology, 2015, 138, 390-396.	7.2	27
65	Effects of volatile–char interactions on in-situ destruction of nascent tar during the pyrolysis and gasification of biomass. Part II. Roles of steam. Fuel, 2015, 143, 555-562.	6.4	68
66	Biomass-derived sugars and furans: Which polymerize more during their hydrolysis?. Fuel Processing Technology, 2015, 137, 212-219.	7.2	64
67	Changes in char reactivity due to char–oxygen and char–steam reactions using victorian brown coal in a fixed-bed reactor. Chinese Journal of Chemical Engineering, 2015, 23, 321-325.	3.5	7
68	Importance of the aromatic structures in volatiles to the in-situ destruction of nascent tar during the volatile–char interactions. Fuel Processing Technology, 2015, 132, 31-38.	7.2	38
69	Changes in nascent char structure during the gasification of low-rank coals in CO2. Fuel, 2015, 158, 711-718.	6.4	36
70	Second-order Raman spectroscopy of char during gasification. Fuel Processing Technology, 2015, 135, 105-111.	7.2	32
71	Formation of nascent char structure during the fast pyrolysis of mallee wood and low-rank coals. Fuel, 2015, 150, 486-492.	6.4	34
72	Effects of CO2 and heating rate on the characteristics of chars prepared in CO2 and N2 atmospheres. Fuel, 2015, 142, 243-249.	6.4	65

#	Article	IF	CITATIONS
73	Upgrading biomass-derived furans via acid-catalysis/hydrogenation: the remarkable difference between water and methanol as the solvent. Green Chemistry, 2015, 17, 219-224.	9.0	98
74	Acid-catalyzed conversion of C6 sugar monomer/oligomers to levulinic acid in water, tetrahydrofuran and toluene: Importance of the solvent polarity. Fuel, 2015, 141, 56-63.	6.4	64
75	Inhibiting and other effects of hydrogen during gasification: Further insights from FT-Raman spectroscopy. Fuel, 2014, 116, 1-6.	6.4	42
76	Microchanneled anode supports of solid oxide fuel cells. Electrochemistry Communications, 2014, 42, 64-67.	4.7	30
77	Effects of gasification atmosphere and temperature on char structural evolution during the gasification of Collie sub-bituminous coal. Fuel, 2014, 117, 1190-1195.	6.4	115
78	Improvement of oxygen permeation through microchanneled ceramic membranes. Journal of Membrane Science, 2014, 454, 444-450.	8.2	24
79	Effects of volatile–char interactions on in situ destruction of nascent tar during the pyrolysis and gasification of biomass. Part I. Roles of nascent char. Fuel, 2014, 122, 60-66.	6.4	91
80	Hierarchically structured NiO/CeO2 nanocatalysts templated by eggshell membranes for methane steam reforming. Catalysis Today, 2014, 228, 199-205.	4.4	21
81	Upgrading of bio-oil into advanced biofuels and chemicals. Part III. Changes in aromatic structure and coke forming propensity during the catalytic hydrotreatment of a fast pyrolysis bio-oil with Pd/C catalyst. Fuel, 2014, 116, 642-649.	6.4	71
82	Quantification of strong and weak acidities in bio-oil via non-aqueous potentiometric titration. Fuel, 2014, 115, 652-657.	6.4	28
83	Microstructure control of oxygen permeation membranes with templated microchannels. Journal of Materials Chemistry A, 2014, 2, 410-417.	10.3	40
84	Acid-Catalyzed Conversion of Xylose in 20 Solvents: Insight into Interactions of the Solvents with Xylose, Furfural, and the Acid Catalyst. ACS Sustainable Chemistry and Engineering, 2014, 2, 2562-2575.	6.7	157
85	Effect of Cellulose Crystallinity on Solid/Liquid Phase Reactions Responsible for the Formation of Carbonaceous Residues during Pyrolysis. Industrial & Engineering Chemistry Research, 2014, 53, 2940-2955.	3.7	56
86	Raman Spectroscopic Investigations into Links between Intrinsic Reactivity and Char Chemical Structure. Energy & Fuels, 2014, 28, 285-290.	5.1	64
87	A preliminary Raman spectroscopic perspective for the roles of catalysts during char gasification. Fuel, 2014, 121, 165-172.	6.4	56
88	Catalytic reforming of tar during gasification. Part V. Decomposition of NO precursors on the char-supported iron catalyst. Fuel, 2014, 116, 19-24.	6.4	28
89	Acid-treatment of C5 and C6 sugar monomers/oligomers: Insight into their interactions. Fuel Processing Technology, 2014, 126, 315-323.	7.2	31
90	Polymerization on heating up of bioâ€oil: A model compound study. AICHE Journal, 2013, 59, 888-900.	3.6	150

6

#	Article	IF	CITATIONS
91	Fibrous NiO/CeO <sub>2</sub> nanocatalysts for the partial oxidation of methane at microsecond contact times. RSC Advances, 2013, 3, 1341-1345.	3.6	16
92	Importance of volatile–char interactions during the pyrolysis and gasification of low-rank fuels – A review. Fuel, 2013, 112, 609-623.	6.4	258
93	An advanced biomass gasification technology with integrated catalytic hot gas cleaning. Part II: Tar reforming using char as a catalyst or as a catalyst support. Fuel, 2013, 112, 646-653.	6.4	108
94	Cathode Supports of SOFCs with a Hierarchical Pore Structure. ECS Transactions, 2013, 57, 555-560.	0.5	0
95	FT-IR carbonyl bands of bio-oils: Importance of water. Fuel, 2013, 112, 596-598.	6.4	9
96	One-Pot Synthesis of Levulinic Acid/Ester from C5 Carbohydrates in a Methanol Medium. ACS Sustainable Chemistry and Engineering, 2013, 1, 1593-1599.	6.7	100
97	A microchanneled ceramic membrane for highly efficient oxygen separation. Journal of Materials Chemistry A, 2013, 1, 9641.	10.3	37
98	Effects of gasifying agent on the evolution of char structure during the gasification of Victorian brown coal. Fuel, 2013, 103, 22-28.	6.4	168
99	Catalytic steam reforming of cellulose-derived compounds using a char-supported iron catalyst. Fuel Processing Technology, 2013, 116, 234-240.	7.2	65
100	Catalytic reforming of tar during gasification. Part IV. Changes in the structure of char in the char in the char-supported iron catalyst during reforming. Fuel, 2013, 106, 858-863.	6.4	57
101	A study on carbon formation over fibrous NiO/CeO2 nanocatalysts during dry reforming of methane. Catalysis Today, 2013, 216, 44-49.	4.4	33
102	Effect of sulfuric acid on the pyrolysis of Douglas fir and hybrid poplar wood: Py-GC/MS and TG studies. Journal of Analytical and Applied Pyrolysis, 2013, 104, 117-130.	5.5	49
103	Evolution of aromatic structures during the reforming of bio-oil: Importance of the interactions among bio-oil components. Fuel, 2013, 111, 805-812.	6.4	37
104	Effects of temperature on the yields and properties of bio-oil from the fast pyrolysis of mallee bark. Fuel, 2013, 108, 400-408.	6.4	68
105	Dual bed pyrolysis gasification of coal: Process analysis and pilot test. Fuel, 2013, 112, 624-634.	6.4	38
106	Acid-catalyzed conversion of mono- and poly-sugars into platform chemicals: Effects of molecular structure of sugar substrate. Bioresource Technology, 2013, 133, 469-474.	9.6	62
107	Investigation of deactivation mechanisms of a solid acid catalyst during esterification of the bio-oils from mallee biomass. Applied Energy, 2013, 111, 94-103.	10.1	51
108	Upgrading of bio-oil into advanced biofuels and chemicals. Part I. Transformation of GC-detectable light species during the hydrotreatment of bio-oil using Pd/C catalyst. Fuel, 2013, 111, 709-717.	6.4	73

#	Article	IF	CITATIONS
109	Formation of coke during the pyrolysis of bio-oil. Fuel, 2013, 108, 439-444.	6.4	91
110	An advanced biomass gasification technology with integrated catalytic hot gas cleaning. Fuel, 2013, 108, 409-416.	6.4	52
111	Upgrading of bio-oil into advanced biofuels and chemicals. Part II. Importance of holdup of heavy species during the hydrotreatment of bio-oil in a continuous packed-bed catalytic reactor. Fuel, 2013, 112, 302-310.	6.4	65
112	Coproduction of clean syngas and iron from woody biomass and natural goethite ore. Fuel, 2013, 103, 64-72.	6.4	23
113	Mechanisms and kinetic modelling of steam gasification of brown coal in the presence of volatile–char interactions. Fuel, 2013, 103, 7-13.	6.4	55
114	Effect of sulfuric acid concentration on the yield and properties of the bio-oils obtained from the auger and fast pyrolysis of Douglas Fir. Fuel, 2013, 104, 536-546.	6.4	76
115	Effect of sulfuric acid addition on the yield and composition of lignin derived oligomers obtained by the auger and fast pyrolysis of Douglas-fir wood. Fuel, 2013, 103, 512-523.	6.4	40
116	Catalytic reforming of tar during gasification. Part III. Effects of feedstock on tar reforming using ilmenite as a catalyst. Fuel, 2013, 103, 950-955.	6.4	33
117	Acid-catalysed treatment of the mallee leaf bio-oil with methanol: Effects of molecular structure of carboxylic acids and esters on their conversion. Fuel Processing Technology, 2013, 106, 569-576.	7.2	24
118	Transformation of chlorine in NaCl-loaded Victorian brown coal during the gasification in steam. Journal of Fuel Chemistry and Technology, 2012, 40, 1409-1414.	2.0	7
119	Changes in Char Structure during the Gasification of Mallee Wood: Effects of Particle Size and Steam Supply. Energy & Fuels, 2012, 26, 193-198.	5.1	24
120	Formation of Aromatic Structures during the Pyrolysis of Bio-oil. Energy & amp; Fuels, 2012, 26, 241-247.	5.1	132
121	2011 Sino-Australian Symposium on Advanced Coal and Biomass Utilisation Technologies. Energy & Fuels, 2012, 26, 1-3.	5.1	7
122	Mediating acid-catalyzed conversion of levoglucosan into platform chemicals with various solvents. Green Chemistry, 2012, 14, 3087.	9.0	74
123	Esterification of bio-oil from mallee (Eucalyptus loxophleba ssp. gratiae) leaves with a solid acid catalyst: Conversion of the cyclic ether and terpenoids into hydrocarbons. Bioresource Technology, 2012, 123, 249-255.	9.6	26
124	Yield and properties of bio-oil from the pyrolysis of mallee leaves in a fluidised-bed reactor. Fuel, 2012, 102, 506-513.	6.4	28
125	Formation of carbon on non-porous Ni mesh during the catalytic pyrolysis of acetylene. Fuel Processing Technology, 2012, 104, 319-324.	7.2	4
126	Novel CO <sub>2</sub> -tolerant ion-transporting ceramic membranes with an external short circuit for oxygen separation at intermediate temperatures. Energy and Environmental Science, 2012, 5, 5257-5264.	30.8	78

#	Article	IF	CITATIONS
127	Production of value-added chemicals from bio-oil via acid catalysis coupled with liquid–liquid extraction. RSC Advances, 2012, 2, 9366.	3.6	65
128	Acid atalyzed Conversion of Xylose in Methanolâ€Rich Medium as Part of Biorefinery. ChemSusChem, 2012, 5, 1427-1434.	6.8	83
129	Hydrolysis and glycosidation of sugars during the esterification of fast pyrolysis bio-oil. Fuel, 2012, 95, 146-151.	6.4	43
130	Acid-catalysed reactions between methanol and the bio-oil from the fast pyrolysis of mallee bark. Fuel, 2012, 97, 512-522.	6.4	70
131	Effect of pyrolysis temperature on the yield and properties of bio-oils obtained from the auger pyrolysis of Douglas Fir wood. Journal of Analytical and Applied Pyrolysis, 2012, 93, 52-62.	5.5	94
132	Poly(furfuryl alcohol)-assisted pyrolysis synthesis of ceramic nanoparticles for solid oxide fuel cells. Materials Research Bulletin, 2012, 47, 1661-1665.	5.2	0
133	Reforming of Volatiles from the Biomass Pyrolysis over Charcoal in a Sequence of Coke Deposition and Steam Gasification of Coke. Energy & amp; Fuels, 2011, 25, 5387-5393.	5.1	77
134	Effect of Coal Drying on the Behavior of Inorganic Species during Victorian Brown Coal Pyrolysis and Combustion. Energy & amp; Fuels, 2011, 25, 2764-2771.	5.1	16
135	Biochar as a Fuel: 3. Mechanistic Understanding on Biochar Thermal Annealing at Mild Temperatures and Its Effect on Biochar Reactivity. Energy & Fuels, 2011, 25, 406-414.	5.1	56
136	Levulinic esters from the acid-catalysed reactions of sugars and alcohols as part of a bio-refinery. Green Chemistry, 2011, 13, 1676.	9.0	200
137	Eggshell membrane-templated synthesis of highly crystalline perovskite ceramics for solid oxidefuelcells. Journal of Materials Chemistry, 2011, 21, 1028-1032.	6.7	39
138	Removal and Recycling of Inherent Inorganic Nutrient Species in Mallee Biomass and Derived Biochars by Water Leaching. Industrial & Engineering Chemistry Research, 2011, 50, 12143-12151.	3.7	130
139	A 3D fibrous cathode with high interconnectivity for solid oxide fuel cells. Electrochemistry Communications, 2011, 13, 1038-1041.	4.7	21
140	Catalytic oxidation of ethane with oxygen using fluidised nanoparticle NiO catalyst. Applied Catalysis A: General, 2011, 405, 166-174.	4.3	20
141	An FT-IR spectroscopic study of carbonyl functionalities in bio-oils. Fuel, 2011, 90, 3417-3423.	6.4	159
142	Reaction pathways of glucose during esterification: Effects of reaction parameters on the formation of humin type polymers. Bioresource Technology, 2011, 102, 10104-10113.	9.6	140
143	A mechanistic study on kinetic compensation effect during low-temperature oxidation of coal chars. Proceedings of the Combustion Institute, 2011, 33, 1755-1762.	3.9	60
144	Effects of crystallite size on the kinetics and mechanism of NiO reduction with H <sub>2</sub> . International Journal of Chemical Kinetics, 2011, 43, 667-676.	1.6	13

#	Article	IF	CITATIONS
145	NiO reduction with hydrogen and light hydrocarbons: Contrast between SiO2-supported and unsupported NiO nanoparticles. Applied Catalysis A: General, 2011, 398, 187-194.	4.3	23
146	Volatilisation and catalytic effects of alkali and alkaline earth metallic species during the pyrolysis and gasification of Victorian brown coal. Part IX. Effects of volatile-char interactions on char–H2O and char–O2 reactivities. Fuel, 2011, 90, 1655-1661.	6.4	77
147	Effects of volatile–char interactions on the evolution of char structure during the gasification of Victorian brown coal in steam. Fuel, 2011, 90, 1529-1535.	6.4	156
148	Catalytic reforming of tar during gasification. Part I. Steam reforming of biomass tar using ilmenite as a catalyst. Fuel, 2011, 90, 1847-1854.	6.4	162
149	Experimental investigation of the combustion of bituminous coal in air and O2/CO2 mixtures: 2. Variation of the transformation behaviour of mineral matter with bulk gas composition. Fuel, 2011, 90, 1361-1369.	6.4	18
150	Simultaneous catalytic esterification of carboxylic acids and acetalisation of aldehydes in a fast pyrolysis bio-oil from mallee biomass. Fuel, 2011, 90, 2530-2537.	6.4	92
151	Catalytic reforming of tar during gasification. Part II. Char as a catalyst or as a catalyst support for tar reforming. Fuel, 2011, 90, 2545-2552.	6.4	212
152	Mallee wood fast pyrolysis: Effects of alkali and alkaline earth metallic species on the yield and composition of bio-oil. Fuel, 2011, 90, 2915-2922.	6.4	273
153	Synthesis and characterization of doped La9ASi6O26.5 (AÂ=ÂCa, Sr, Ba) oxyapatite electrolyte by a water-based gel-casting route. International Journal of Hydrogen Energy, 2011, 36, 6862-6874.	7.1	49
154	Evolution of organically bound metals during coal combustion in air and O2/CO2 mixtures: A case study of Victorian brown coal. Proceedings of the Combustion Institute, 2011, 33, 2795-2802.	3.9	15
155	In-situ observation of the combustion of air-dried and wet Victorian brown coal. Proceedings of the Combustion Institute, 2011, 33, 1739-1746.	3.9	43
156	Combustion synthesis of ceramic nanoparticles for solid oxide fuel cells. Asia-Pacific Journal of Chemical Engineering, 2010, 5, 593-598.	1.5	3
157	Formation of NOx precursors during the pyrolysis of coal and biomass. Part X: Effects of volatile–char interactions on the conversion of coal-N during the gasification of a Victorian brown coal in O2 and steam at 800°C. Fuel, 2010, 89, 1035-1040.	6.4	15
158	In situ diagnostics of Victorian brown coal combustion in O2/N2 and O2/CO2 mixtures in drop-tube furnace. Fuel, 2010, 89, 2703-2712.	6.4	106
159	An investigation of the causes of the difference in coal particle ignition temperature between combustion in air and in O2/CO2. Fuel, 2010, 89, 3381-3387.	6.4	90
160	Influences of minerals transformation on the reactivity of high temperature char gasification. Fuel Processing Technology, 2010, 91, 404-409.	7.2	36
161	Evaluation of structural features of chars from pyrolysis of biomass of different particle sizes. Fuel Processing Technology, 2010, 91, 877-881.	7.2	106
162	Production and fuel properties of fast pyrolysis oil/bio-diesel blends. Fuel Processing Technology, 2010, 91, 296-305.	7.2	104

#	Article	IF	CITATIONS
163	Changes in char reactivity and structure during the gasification of a Victorian brown coal: Comparison between gasification in O2 and CO2. Fuel Processing Technology, 2010, 91, 800-804.	7.2	88
164	Effects of biomass char structure on its gasification reactivity. Bioresource Technology, 2010, 101, 7935-7943.	9.6	202
165	Separation, hydrolysis and fermentation of pyrolytic sugars to produce ethanol and lipids. Bioresource Technology, 2010, 101, 9688-9699.	9.6	192
166	Catalytic and Noncatalytic Mechanisms in Steam Gasification of Char from the Pyrolysis of Biomass <sup>â€</sup> . Energy & Fuels, 2010, 24, 108-116.	5.1	126
167	HCN and NH <sub>3</sub> Formation during Coal/Char Gasification in the Presence of NO. Environmental Science & Technology, 2010, 44, 3719-3723.	10.0	27
168	Characteristics of Gas-Phase Partial Oxidation of Nascent Tar from the Rapid Pyrolysis of Cedar Sawdust at 700â ``800 °C. Energy & Fuels, 2010, 24, 2900-2909.	5.1	21
169	In-Situ Reforming of Tar from the Rapid Pyrolysis of a Brown Coal over Char <sup>â€</sup> . Energy & Fuels, 2010, 24, 76-83.	5.1	74
170	High-Speed Camera Observation of Coal Combustion in Air and O <sub>2</sub> /CO <sub>2</sub> Mixtures and Measurement of Burning Coal Particle Velocity <sup>â€</sup> . Energy & Fuels, 2010, 24, 29-37.	5.1	48
171	Bioslurry as a Fuel. 3. Fuel and Rheological Properties of Bioslurry Prepared from the Bio-oil and Biochar of Mallee Biomass Fast Pyrolysis. Energy & Fuels, 2010, 24, 5669-5676.	5.1	59
172	Experimental Investigation of the Combustion of Bituminous Coal in Air and O <sub>2</sub> /CO <sub>2</sub> Mixtures: 1. Particle Imaging of the Combustion of Coal and Char. Energy & Fuels, 2010, 24, 4803-4811.	5.1	19
173	Thermosetting polymer templated nanoporous sinter-active layer for low temperature solid oxidefuelcells. Journal of Materials Chemistry, 2010, 20, 1122-1126.	6.7	17
174	Polymer hydrogel assisted combustion synthesis of highly crystalline ceramic nanoparticles for SOFC electrolyte films. Materials Chemistry and Physics, 2009, 118, 148-152.	4.0	9
175	Influence of coal blending on mineral transformation at high temperatures. Mining Science and Technology, 2009, 19, 300-305.	0.3	5
176	Influences of mineral matter on high temperature gasification of coal char. Journal of Fuel Chemistry and Technology, 2009, 37, 134-138.	2.0	29
177	Effects of particle size on the fast pyrolysis of oil mallee woody biomass. Fuel, 2009, 88, 1810-1817.	6.4	307
178	Positive and negative catalytic effects of a nickel mesh catalyst for the partial oxidation of ethane. Chemical Engineering Journal, 2009, 147, 307-315.	12.7	10
179	Catalytic Reactions of Ethylene and Hydrogen in a Fluidized-Bed Reactor with Ni Nanoparticles. Energy & Fuels, 2009, 23, 4866-4870.	5.1	5
180	Mallee Biomass as a Key Bioenergy Source in Western Australia: Importance of Biomass Supply Chain. Energy & Fuels, 2009, 23, 3290-3299.	5.1	75

#	Article	IF	CITATIONS
181	Importance of Biomass Particle Size in Structural Evolution and Reactivity of Char in Steam Gasification. Industrial & Engineering Chemistry Research, 2009, 48, 9858-9863.	3.7	36
182	Rapid Gasification of Nascent Char in Steam Atmosphere during the Pyrolysis of Na- and Ca-Ion-Exchanged Brown Coals in a Drop-Tube Reactor. Energy & Fuels, 2009, 23, 4496-4501.	5.1	18
183	Evolution of Char Structure during the Steam Gasification of Biochars Produced from the Pyrolysis of Various Mallee Biomass Components. Industrial & Engineering Chemistry Research, 2009, 48, 10431-10438.	3.7	106
184	Shape forming of ceramics with controllable microstructure by drying-free colloidal casting. Journal of Materials Chemistry, 2009, 19, 7070.	6.7	9
185	Opposite effects of gas flow rate on the rate of formation of carbon during the pyrolysis of ethane and acetylene on a nickel mesh catalyst. Carbon, 2008, 46, 1208-1217.	10.3	28
186	Effects of volatile–char interactions on the volatilisation of alkali and alkaline earth metallic species during the pyrolysis of biomass. Fuel, 2008, 87, 1187-1194.	6.4	106
187	Drastic changes in biomass char structure and reactivity upon contact with steam. Fuel, 2008, 87, 1127-1132.	6.4	127
188	NH3 and HCN formation during the gasification of three rank-ordered coals in steam and oxygen. Fuel, 2008, 87, 1102-1107.	6.4	29
189	Mechanism of decomposition of aromatics over charcoal and necessary condition for maintaining its activity. Fuel, 2008, 87, 2914-2922.	6.4	134
190	Evolution of biomass char structure during oxidation in O2 as revealed with FT-Raman spectroscopy. Fuel Processing Technology, 2008, 89, 1429-1435.	7.2	89
191	Effects of Temperature on the Formation of Lignin-Derived Oligomers during the Fast Pyrolysis of Mallee Woody Biomass. Energy & Fuels, 2008, 22, 2022-2032.	5.1	207
192	Fast Pyrolysis of Oil Mallee Woody Biomass:  Effect of Temperature on the Yield and Quality of Pyrolysis Products. Industrial & Engineering Chemistry Research, 2008, 47, 1846-1854.	3.7	323
193	Changes in Char Structure during the Gasification of a Victorian Brown Coal in Steam and Oxygen at 800 ŰC. Energy & Fuels, 2008, 22, 4034-4038.	5.1	95
194	Activity of Mesoporous Alumina Particles for Biomass Steam Reforming in a Fluidized-Bed Reactor and Its Application to a Dual-Gas-Flow Two-Stage Reactor System. Industrial & Engineering Chemistry Research, 2008, 47, 5346-5352.	3.7	16
195	Effects of Dewatering on the Pyrolysis and Gasification Reactivity of Victorian Brown Coalâ€. Energy & Fuels, 2007, 21, 399-404.	5.1	24
196	An incentive mechanism for message relaying in unstructured peer-to-peer systems. , 2007, , .		15
197	Characterization of the Structural Features of Char from the Pyrolysis of Cane Trash Using Fourier Transformâ^'Raman Spectroscopy. Energy & Fuels, 2007, 21, 1816-1821.	5.1	106
198	Behavior of Inherent Metallic Species as a Crucial Factor for Kinetics of Steam Gasification of Char from Coal Pyrolysisâ€. Energy & Fuels, 2007, 21, 387-394.	5.1	42

#	Article	IF	CITATIONS
199	Novel Waterâ^'Gas-Shift Reaction Catalyst from Iron-Loaded Victorian Brown Coalâ€. Energy & Fuels, 2007, 21, 395-398.	5.1	12
200	Conversion of Fuel-N into HCN and NH3During the Pyrolysis and Gasification in Steam:Â A Comparative Study of Coal and Biomassâ€. Energy & Fuels, 2007, 21, 517-521.	5.1	132
201	NH3Formation and Destruction during the Gasification of Coal in Oxygen and Steam. Environmental Science & Comp. Technology, 2007, 41, 5505-5509.	10.0	35
202	Coke formation and reaction pathways of catalyst-surface-generated radicals during the pyrolysis of ethane using Ni mesh catalyst. Applied Catalysis A: General, 2007, 316, 90-99.	4.3	31
203	Some recent advances in the understanding of the pyrolysis and gasification behaviour of Victorian brown coal. Fuel, 2007, 86, 1664-1683.	6.4	433
204	Examination of catalytic roles of inherent metallic species in steam reforming of nascent volatiles from the rapid pyrolysis of a brown coal. Fuel Processing Technology, 2007, 88, 179-185.	7.2	32
205	Humic Acids as a Complexible Fuel for Combustion Synthesis of Ceramic Nanoparticles. Journal of the American Ceramic Society, 2007, 90, 4012-4014.	3.8	4
206	Interparticle Desorption and Re-adsorption of Alkali and Alkaline Earth Metallic Species within a Bed of Pyrolyzing Char from Pulverized Woody Biomass. Energy & Fuels, 2006, 20, 1294-1297.	5.1	38
207	Effects of Pretreatment in Steam on the Pyrolysis Behavior of Loy Yang Brown Coal. Energy & Fuels, 2006, 20, 281-286.	5.1	41
208	Formation of HCN and NH3during the Reforming of Quinoline with Steam in a Fluidized-bed Reactor. Energy & Fuels, 2006, 20, 159-163.	5.1	12
209	Effect of iron on the gasification of Victorian brown coal with steam:enhancement of hydrogen production. Fuel, 2006, 85, 127-133.	6.4	95
210	Inhibition of steam gasification of char by volatiles in a fluidized bed under continuous feeding of a brown coal. Fuel, 2006, 85, 340-349.	6.4	105
211	Volatilisation and catalytic effects of alkali and alkaline earth metallic species during the pyrolysis and gasification of Victorian brown coal. Part VIII. Catalysis and changes in char structure during gasification in steam. Fuel, 2006, 85, 1518-1525.	6.4	148
212	Formation of NOx precursors during the pyrolysis of coal and biomass. Part IX. Effects of coal ash and externally loaded-Na on fuel-N conversion during the reforming of coal and biomass in steam. Fuel, 2006, 85, 1411-1417.	6.4	29
213	Volatilisation and catalytic effects of alkali and alkaline earth metallic species during the pyrolysis and gasification of Victorian brown coal. Part VII. Raman spectroscopic study on the changes in char structure during the catalytic gasification in air. Fuel, 2006, 85, 1509-1517.	6.4	202
214	FT-Raman spectroscopic study of the evolution of char structure during the pyrolysis of a Victorian brown coal. Fuel, 2006, 85, 1700-1707.	6.4	767
215	Effects of volatile–char interaction on the formation of HCN and NH3 during the gasification of Victorian brown coal in O2 at 500°C. Fuel, 2006, 85, 2148-2154.	6.4	18
216	Char-Supported Nano Iron Catalyst for Water-Gas-Shift Reaction. Chemical Engineering Research and Design, 2006, 84, 125-130.	5.6	67

#	Article	IF	CITATIONS
217	Special Issue—Gasification: a Route to Clean Energy. Chemical Engineering Research and Design, 2006, 84, 407-408.	5.6	44
218	Effects of volatile–char interactions on the reactivity of chars from NaCl-loaded Loy Yang brown coal. Fuel, 2005, 84, 1221-1228.	6.4	77
219	Formation of NO precursors during the pyrolysis of coal and biomass. Part VII. Pyrolysis and gasification of cane trash with steam. Fuel, 2005, 84, 371-376.	6.4	52
220	Kinetics of steam gasification of nascent char from rapid pyrolysis of a Victorian brown coal. Fuel, 2005, 84, 1612-1612.	6.4	65
221	Effects of thermal pretreatment in helium on the pyrolysis behaviour of Loy Yang brown coal. Fuel, 2005, 84, 1586-1586.	6.4	30
222	Formation of NO precursors during the pyrolysis of coal and biomass. Part VIII. Effects of pressure on the formation of NH and HCN during the pyrolysis and gasification of Victorian brown coal in steam. Fuel, 2005, 84, 2102-2108.	6.4	40
223	Volatilisation of alkali and alkaline earth metallic species during the gasification of a Victorian brown coal in CO2. Fuel Processing Technology, 2005, 86, 1241-1251.	7.2	58
224	Volatilisation of alkali and alkaline earth metallic species during the pyrolysis of biomass: differences between sugar cane bagasse and cane trash. Bioresource Technology, 2005, 96, 1570-1577.	9.6	151
225	Spontaneous Generation of Tar Decomposition Promoter in a Biomass Steam Reformer. Chemical Engineering Research and Design, 2005, 83, 1093-1102.	5.6	64
226	Primary Release of Alkali and Alkaline Earth Metallic Species during the Pyrolysis of Pulverized Biomass. Energy & Fuels, 2005, 19, 2164-2171.	5.1	186
227	Structure and Properties of Victorian Brown Coal. , 2004, , 11-84.		25
228	Conversion of Coal-N and Coal-S during Pyrolysis, Gasification and Combustion. , 2004, , 286-359.		4
229	Pyrolysis of a Victorian brown coal and gasification of nascent char in CO2 atmosphere in a wire-mesh reactor. Fuel, 2004, 83, 833-843.	6.4	141
230	Volatilisation and catalytic effects of alkali and alkaline earth metallic species during the pyrolysis and gasification of Victorian brown coal. Part VI. Further investigation into the effects of volatile-char interactions. Fuel, 2004, 83, 1273-1279.	6.4	90
231	Release of fuel-nitrogen during the gasification of Shenmu coal in O2. Fuel Processing Technology, 2004, 85, 1053-1063.	7.2	21
232	Volatilisation and catalytic effects of alkali and alkaline earth metallic species during the pyrolysis and gasification of Victorian brown coal. Part V. Combined effects of Na concentration and char structure on char reactivity. Fuel, 2004, 83, 23-30.	6.4	124
233	Evidence of poly-condensed aromatic rings in a Victorian brown coal. Fuel, 2004, 83, 97-107.	6.4	37
234	Roles of desorbed radicals and reaction products during the oxidation of methane using a nickel mesh catalyst. Applied Catalysis A: General, 2004, 258, 63-71.	4.3	20

#	Article	IF	CITATIONS
235	Pyrolysis of liquefied petroleum gas assisted by radicals desorbed from mesh catalyst surface. International Journal of Chemical Kinetics, 2003, 35, 637-646.	1.6	8
236	Combined effects of pressure and ion-exchangeable metallic species on pyrolysis of Victorian lignite. Fuel, 2003, 82, 343-350.	6.4	50
237	Volatilisation and catalytic effects of alkali and alkaline earth metallic species during the pyrolysis and gasification of Victorian brown coal. Part IV. Catalytic effects of NaCl and ion-exchangeable Na in coal on char reactivity⯆. Fuel, 2003, 82, 587-593.	6.4	200
238	Formation of NOx precursors during the pyrolysis of coal and biomass. Part VI. Effects of gas atmosphere on the formation of NH3 and HCNâ~†. Fuel, 2003, 82, 1159-1166.	6.4	93
239	Release of alkali and alkaline earth metallic species during rapid pyrolysis of a Victorian brown coal at elevated pressuresâ~†. Fuel, 2003, 82, 1491-1497.	6.4	66
240	Studies of the release rule of NOx precursors during gasification of coal and its char. Fuel Processing Technology, 2003, 84, 243-254.	7.2	24
241	Effects of radical desorption on catalyst activity and coke formation during the catalytic pyrolysis and oxidation of light alkanes. Applied Catalysis A: General, 2003, 250, 83-94.	4.3	17
242	Volatilisation and catalytic effects of alkali and alkaline earth metallic species during the pyrolysis and gasification of Victorian brown coal. Part I. Volatilisation of Na and Cl from a set of NaCl-loaded samples. Fuel, 2002, 81, 143-149.	6.4	268
243	Kinetic relationship between NO/N2O reduction and O2 consumption during flue-gas recycling coal combustion in a bubbling fluidized-bed. Fuel, 2002, 81, 1179-1188.	6.4	19
244	Release of volatiles from the pyrolysis of a Victorian lignite at elevated pressures. Fuel, 2002, 81, 1171-1178.	6.4	37
245	Formation of NOx precursors during the pyrolysis of coal and biomass. Part V. Pyrolysis of a sewage sludgeâ <sup>-</sup> †. Fuel, 2002, 81, 2203-2208.	6.4	126
246	Volatilisation and catalytic effects of alkali and alkaline earth metallic species during the pyrolysis and gasification of Victorian brown coal. Part II. Effects of chemical form and valence. Fuel, 2002, 81, 151-158.	6.4	185
247	Volatilisation and catalytic effects of alkali and alkaline earth metallic species during the pyrolysis and gasification of Victorian brown coal. Part III. The importance of the interactions between volatiles and char at high temperature. Fuel, 2002, 81, 1033-1039.	6.4	187
248	Roles of inherent metallic species in secondary reactions of tar and char during rapid pyrolysis of brown coals in a drop-tube reactor. Fuel, 2002, 81, 1977-1987.	6.4	111
249	Interinfluence between Reactions on the Catalyst Surface and Reactions in the Gas Phase during the Catalytic Oxidation of Methane with Air. Journal of Catalysis, 2001, 197, 315-323.	6.2	17
250	Formation of NOx and SOx precursors during the pyrolysis of coal and biomass. Part IV. Pyrolysis of a set of Australian and Chinese coals. Fuel, 2001, 80, 2131-2138.	6.4	75
251	Formation of NOx and SOx precursors during the pyrolysis of coal and biomass. Part III. Further discussion on the formation of HCN and NH3 during pyrolysis. Fuel, 2000, 79, 1899-1906.	6.4	185
252	Formation of NOx and SOx precursors during the pyrolysis of coal and biomass. Part I. Effects of reactor configuration on the determined yields of HCN and NH3 during pyrolysis. Fuel, 2000, 79, 1883-1889.	6.4	122

#	Article	IF	CITATIONS
253	Formation of NOx and SOx precursors during the pyrolysis of coal and biomass. Part II. Effects of experimental conditions on the yields of NOx and SOx precursors from the pyrolysis of a Victorian brown coal. Fuel, 2000, 79, 1891-1897.	6.4	93
254	Fates and roles of alkali and alkaline earth metals during the pyrolysis of a Victorian brown coal. Fuel, 2000, 79, 427-438.	6.4	383
255	Fluorescence Spectroscopic Analysis of Tars from the Pyrolysis of a Victorian Brown Coal in a Wire-Mesh Reactor. Energy & Fuels, 2000, 14, 476-482.	5.1	48
256	Effects of Heating Rate and Ion-Exchangeable Cations on the Pyrolysis Yields from a Victorian Brown Coal. Energy & Fuels, 1999, 13, 748-755.	5.1	183
257	Effects of temperature and molecular mass on the nitrogen functionality of tars produced under high heating rate conditions. Fuel, 1998, 77, 157-164.	6.4	50
258	Cyclopenta-fused polycyclic aromatic hydrocarbons from brown coal pyrolysis. Proceedings of the Combustion Institute, 1998, 27, 1677-1686.	0.3	30
259	Release of HCN, NH3, and HNCO from the Thermal Gas-Phase Cracking of Coal Pyrolysis Tars. Energy & Fuels, 1998, 12, 536-541.	5.1	86
260	Formation of HNCO from the Rapid Pyrolysis of Coals. Energy & amp; Fuels, 1996, 10, 264-265.	5.1	66
261	Fate of Aromatic Ring Systems during Thermal Cracking of Tars in a Fluidized-Bed Reactor. Energy & Fuels, 1996, 10, 1083-1090.	5.1	74
262	Interactions of quartz, zircon sand and stainless steel with ammonia: implications for the measurement of ammonia at high temperatures. Fuel, 1996, 75, 525-526.	6.4	23
263	Loss of cations from brown coals during pyrolysis: partly an analytical artefact?. Fuel, 1996, 75, 780.	6.4	4
264	Impact of temperature and fuel-nitrogen content on fuel-staged combustion with coal pyrolysis gas. Proceedings of the Combustion Institute, 1996, 26, 2231-2239.	0.3	18
265	An experimental study of the release of nitrogen from coals pyrolyzed in fluidized-bed reactors. Proceedings of the Combustion Institute, 1996, 26, 3205-3211.	0.3	26
266	The effects of pyrolysis temperature and ion-exchanged metals on the composition of brown coal tars produced in a fluidized-bed reactor. Proceedings of the Combustion Institute, 1996, 26, 3287-3294.	0.3	13
267	Characterization of successive time/temperature-resolved liquefaction extract fractions released from coal in a flowing-solvent reactor. Fuel, 1995, 74, 37-45.	6.4	57
268	Molecular masses up to 270 000 u in coal and coal-derived products by matrix assisted laser desorption ionization mass spectrometry (MALDI-m.s.). Fuel, 1994, 73, 1606-1616.	6.4	40
269	Liquefaction of coal and maceral concentrates in a stirred micro-autoclave and a flowing-solvent reactor. Fuel, 1994, 73, 1331-1337.	6.4	12
270	Characterization of coal by matrix-assisted laser desorption ionization mass spectrometry. I. The argonne coal samples. Rapid Communications in Mass Spectrometry, 1994, 8, 808-814.	1.5	41

#	Article	IF	CITATIONS
271	Characterization of coal by matrix-assisted laser desorption mass spectrometry. II. Pyrolysis tars and liquefaction extracts from the argonne coal samples. Rapid Communications in Mass Spectrometry, 1994, 8, 815-822.	1.5	42
272	Characterization of kerogens by matrix-assisted laser desorption ionization mass spectroscopy. Rapid Communications in Mass Spectrometry, 1994, 8, 823-828.	1.5	22
273	Comparison of product distributions from the thermal reactions of tetralin in a stirred autoclave and a flowing-solvent reactor. Fuel, 1994, 73, 789-794.	6.4	19
274	Comparison of thermal breakdown in coal pyrolysis and liquefaction. Fuel, 1994, 73, 851-865.	6.4	66
275	Effect of reactor configuration on the yields and structures of pine-wood derived pyrolysis liquids: A comparison between ablative and wire-mesh pyrolysis. Biomass and Bioenergy, 1994, 7, 155-167.	5.7	33
276	Liquefaction of coals and maceral concentrates in a flowing-solvent reactor. International Journal of Energy Research, 1994, 18, 215-222.	4.5	2
277	UV-Fluorescence Spectroscopy of Coal Pyrolysis Tars. Energy & Fuels, 1994, 8, 1039-1048.	5.1	128
278	Characterization of Successive Extract Fractions Released from a Sample of Coal during Liquefaction in a Flowing-Solvent Reactor. Energy & amp; Fuels, 1994, 8, 1360-1369.	5.1	32
279	Vacuum pyrolysis of maceral concentrates in a wire-mesh reactor. Fuel, 1993, 72, 1459-1468.	6.4	90
280	Characterization of tars from variable heating rate pyrolysis of maceral concentrates. Fuel, 1993, 72, 3-11.	6.4	140
281	Effect of H2-pressure on yields and structures of liquids from the hydropyrolysis of maceral concentrates. Fuel Processing Technology, 1993, 36, 327-332.	7.2	5
282	Effect of H2-pressure on the structures of bio-oils from the mild hydropyrolysis of biomass. Biomass and Bioenergy, 1993, 5, 155-171.	5.7	31
283	Carbon clusters from coal-derived materials. Rapid Communications in Mass Spectrometry, 1993, 7, 360-362.	1.5	22
284	Identification of molecular masses up to 270 000 u in coal and coal-derived products by matrix-assisted laser desorption mass spectrometry. Rapid Communications in Mass Spectrometry, 1993, 7, 795-799.	1.5	30
285	Comparison of fast atom bombardment mass spectrometry and size exclusion chromatography in defining high molecular masses in coal-derived materials. Fuel, 1993, 72, 1317-1325.	6.4	26
286	High mass compounds (up to 12000 u) in coal tars. Journal of the Chemical Society Chemical Communications, 1993, , 767.	2.0	16
287	Pyrolysis characteristics of macerals separated from a single coal and their artificial mixture. Fuel, 1991, 70, 474-479.	6.4	33
288	High mass material (>104 daltons) in a coal liquefaction extract, by laser-desorption mass spectrometry. Rapid Communications in Mass Spectrometry, 1991, 5, 364-367.	1.5	32